

COMPONENT PART NOTICE

THIS PAPER IS A COMPONENT PART OF THE FOLLOWING COMPILATION REPORT:

TITLE: Vibration Damping Workshop Proceedings Held at Long Beach, California on
27-29 February 1984.

TO ORDER THE COMPLETE COMPILATION REPORT, USE AD-A152 547

THE COMPONENT PART IS PROVIDED HERE TO ALLOW USERS ACCESS TO INDIVIDUALLY AUTHORED SECTIONS OF PROCEEDING, ANNALS, SYMPOSIA, ETC. HOWEVER, THE COMPONENT SHOULD BE CONSIDERED WITHIN THE CONTEXT OF THE OVERALL COMPILATION REPORT AND NOT AS A STAND-ALONE TECHNICAL REPORT.

THE FOLLOWING COMPONENT PART NUMBERS COMPRISE THE COMPILATION REPORT:

AD#: P004 685 - AD-P004 734 AD#: _____
AD#: _____ AD#: _____
AD#: _____ AD#: _____

This document has been approved for public release and its distribution is unlimited.

DTIC FORM 463
MAR 85

Accession For	
1. THIS GRA&I	<input checked="" type="checkbox"/>
2. THIS TAB	<input type="checkbox"/>
3. Unannounced	<input type="checkbox"/>
4. Identification	<input type="checkbox"/>
5. _____	
6. _____	
Availability Codes	
Dist	Avail and/or Special
4/1	

DTIC
SELECTED
S JUN 27 1985 **D**
A

OPI: DTIC-110

AD-P004 733

FLEXIBLE STRUCTURE CONTROL IN THE FREQUENCY DOMAIN

R. Harding and Dr. A. Das
General Electric Space Division
Spacecraft Operations
Control Systems Design
Philadelphia, Pennsylvania

Flexible Structure Control in the Frequency Domain

R. Harding

Dr. A. Das

General Electric Space Division
Spacecraft Operations
Control Systems Design

Abstract

New techniques to analyze structure and controller interaction in the frequency domain are defined and used to determine the modal damping requirements of the spacecraft structure to assure control system stability and performance. Gain and phase versus frequency (Bode and Nyquist) techniques are described which predict system stability in the presence of uncontrolled structural modes and errors in a priori natural frequencies and quantify control system margin for these modes. The techniques are applied to an optimally controlled single axis satellite with very large solar arrays. Control system actuator and sensor configurations are based upon system controllability and observability of four dominant structural modes. Verification of the techniques is by simulation.



INTRODUCTION

Preliminary analyses of Large Space Structures (LSS) have brought to light difficult problems of designing a control system that has to meet very accurate pointing requirements in the presence of low frequency structural modes. To satisfy pointing accuracy requirements, the bandwidths of the attitude control system (ACS) have to be at least one or two orders of magnitude higher than classical development techniques can provide. Nearly all past and present spacecraft have an ACS with frequency bandwidths which are about 2% of the frequency of the fundamental structural mode. This frequency ratio allows the response of the ACS to be attenuated sharply at frequencies above the bandwidth of the controller through the use of low pass filters.

Higher bandwidths can be achieved for spacecraft with linearizable dynamic systems by optimizing quadratic cost functionals in the presence of gaussian noise. These optimal linearizable quadratic Gaussian (LQG) designs seem to be a good choice, although, they have several drawbacks. The LQG controllers require much greater resources in the onboard computers and can be unstable if the spacecraft have dominant high frequency structural modes not accounted for in the design. Good estimates of the modeshapes, the modal critical damping ratios and the natural frequencies of the spacecraft structure are required for the LQG controllers to be effective. Errors in any of these parameters may result in unstable conditions and necessitate structure redesign, controller redesign, or inclusion of some kind of parameter estimation/correction technique. The LSS trend causes the control and structure frequency spectrums to overlap. Interaction of these disciplines becomes of paramount importance to insure stability as well as to meet structure size, weight, stress and other constraints. Preliminary design will be an extremely dynamic process that must include trades with controller complexity and structure damping design. Active versus passive structure damping is such a trade that is addressed in this paper.

Frequency domain design and analysis for multivariable control problems has been a subject of intense investigation in recent years. Unconditional system stability methods for multivariable control is approached in a variety of ways that include eigenvalue analysis, singular value determination [7], positivity concepts [2], and generalised Nyquist trajectories [6,9]. The approach presented here is pragmatic in that LQG methods are applied to a flexible spacecraft, but, it is also innovative with frequency response analysis techniques that give insight into particular state element sensitivities and stability margins.

SUMMARY

Attitude and flexible mode control of a spacecraft with very large solar arrays is simulated and analyzed for stability in the frequency domain. The LQG controller developed for this investigation uses three torque producing actuators, a rate sensor, an absolute position sensor, and four relative position sensors. The LQG controller actively damps structural modes while causing the attitude transient response settling time to be an order of magnitude faster than the response of a classical controller. Frequency response analyses show the second dominant mode to be notched from the LQG controller response due to that mode's small observability and controllability.

This conclusion is verified by simulation. Adding passive damping to the second dominant mode significantly enhances plant stability margin and decreases solar array transient response settling time. Control spillover analysis is accomplished by adding two uncompensated modes to the true plant system dynamics. Frequency response analysis with simulations show the system to be stable with uncompensated modes even with large errors in a priori structure critical parameters. The frequency response techniques provide a graphic means of measuring stability margins of state elements and prediction of critical parameter errors that can cause instability. Examples of a priori natural frequency error and modal admittance error tolerances are given with results from simulations to validate these assertions.

OPTIMAL CONTROL SYNTHESIS

Most previous satellite controller designs have been able to meet the performance specification while avoiding active control of any structural mode. The standard design procedure rolls off the controller response at higher frequencies so that the system response is highly attenuated at the modal natural frequencies. Avoiding these modes while increasing the bandwidth of the controller requires additional compensation for notching the controller at the structure natural frequencies. A quadratic performance index optimization method that allows the designer to choose the states to be controlled has gained widespread appreciation as an alternative to the classical approach. This LQG design approach leads to optimal state estimation and the control gains based upon a weighting of the state elements and control effort. In this manner, identifiable structural modes can be included in the controller instead of avoided as in the case of a classical control design. This type control will actively damp controllable and observable modes and enhance attitude control performance. Development of an LQG controller is outlined in the following paragraphs.

A linear time-invariant system can be represented in the form

$$\dot{x} = Ax + Bu + w$$

$$y = Cx + v$$

where,

A = nxn system matrix

B = nxr control matrix

C = mxn measurement matrix

x = nx1 state vector

y = mx1 sensor output vector

u = r1 control vector

w = nx1 noise vector

v = $m \times 1$ measurement noise vector

n = number of states

r = number of actuators

m = number of sensors

The controller is designed based on estimates of A, B, C , and x so the equations for the LQG design become

$$\dot{\hat{x}} = \hat{A}x + \hat{B}u + w$$

$$y = \hat{C}x + v$$

where, $\hat{}$, signifies an estimated entity and w and v are uncorrelated white noise vectors with zero mean. Detailed information for minimizing a scalar performance index as a function of the weighted norm of the state and control effort can be found in several optimization texts [3,8,10]. Minimizing the performance index leads to an optimal control law

$$u(t) = K_1(t)\hat{x}(t) \quad (1)$$

where K_1 is $r \times n$ optimal gain matrix which is found via the following relation.

$$K_1(t) = -R^{-1}(t)\hat{B}^T(t)P_1(t) \quad (2)$$

The $P_1(t)$ matrix is obtained by solving the backward matrix Riccati Equation given by

$$\dot{P}_1(t) = -P_1(t)\hat{A}(t) - \hat{A}^T(t)P_1(t) + P_1(t)\hat{B}(t)R^{-1}(t)\hat{B}^T(t)P_1(t) - Q_1(t) \quad (3)$$

where,

R = constant $m \times m$ control weighting matrix

Q_1 = constant $\hat{n} \times \hat{n}$ control error weighting matrix

\hat{n} = number of estimated states

In a similar fashion, the optimal state estimate, \hat{x} , is found by solving the following equation.

$$\dot{\hat{x}} = \hat{A}\hat{x} + \hat{B}u + K_2(y - \hat{C}\hat{x}) \quad (4)$$

The optimal estimation gains, K_2 , are found via

$$K_2(t) = P_2(t)\hat{C}^T(t)R_2^{-1}(t) \quad (5)$$

and P_2 is found by solving the forward matrix Riccati equation

$$\dot{P}_2(t) = \hat{A}(t)P_2(t) + P_2(t)\hat{A}^T(t) - P_2(t)\hat{C}^T(t)R_2^{-1}(t)\hat{C}(t)P_2(t) + Q_2(t) \quad (6)$$

where,

R_2 = constant $m \times m$ measurement noise covariance matrix

Q_2 = constant $\hat{n} \times \hat{n}$ state noise covariance matrix

The matrix Riccati equations, (3) and (6), are integrated until P_1 and P_2 reach steady state values. Due to nonlinearities of these equations, it is useful to transform (3) and (6) to a set of linear equations to expedite their solutions [8].

REDUCED ORDER MODEL

Truncation of the structural modes to only those modes that must be controlled is very important in order to minimize onboard processing. However, a robust controller must include all dominant modes in its state space, otherwise instabilities may result. Truncation of an infinite set of structural modes to a reduced order model (ROM) is based upon the determination of the dominant modes which will yield maximum deflections for a given input. The following equation facilitates dominant mode identification.

$$\frac{\theta_{m,i}}{f_m} = \frac{\phi_i^2}{2\zeta_i \omega_{n,i}} \quad (7)$$

where,

$\theta_{m,i}$ = maximum deflection at the actuator due to the i th mode

f_m = max torque of the actuator

ϕ_i = modal admittance at the actuator of the i th mode

ζ_i = critical damping ratio for i th mode

$\omega_{n,i}$ = natural frequency for i th mode

Equation (7) relates maximum modal deflection for a maximum input torque. The greatest structural deflections are due to the modes with the largest modeshapes at the lowest frequencies. The first thirty modes for the structure considered are generated from a finite element computer program. The rigid body states and four out of the thirty computed modeshapes comprise the ROM. The four dominant modes and natural frequencies are

First Symmetric Bending (.0407 Hz)

First Asymmetric Bending (.0904 Hz)

Second Asymmetric Bending (.1500 Hz)

Third Asymmetric Bending (.2212 Hz)

Two additional modes are used in the truth model for spillover investigation. Their maximum deflections are at least one order of magnitude less than the four dominant modes and, therefore, not included in the ROM controller. These two uncontrolled or residual modes are

Second Symmetric Bending (.0957 Hz)

Third Symmetric Bending (.1641 Hz)

The capability of the controller to maintain attitude and modal control without knowledge of residual modes is one aspect of the robustness of the system in the presence of destabilizing factors. All structural modes respond in varying degrees to an actuating input, but, a robust controller does not excite residual modes to the point of instability. Instead, it ignores these modes allowing the structure to damp their response. To date, as many as four residual modes have been included in the true plant and results from simulations show only slight performance degradation.

CONTROLLABILITY AND OBSERVABILITY

Actuator and sensor configurations also have a large impact on the controller performance and stability. System observability and controllability must be investigated when designing any control system to insure that the controlled and estimated states adequately span the true state space. Several methods to check for system observability and controllability give go/no-go type information but do not necessarily indicate one configuration as better or worse than another. This investigation applies two different approaches to define the sensor and actuator configurations. One approach maximizes the determinant of the observability and controllability Gramian matrices as a quantitative configuration selection criteria. The other approach maximizes the real part of the eigenvalues for the closed loop estimator and controller. Both methods evaluate various number and locations of torque producing actuators and various number, location, and type of sensors.

Briefly, observability and controllability Gramian matrices are defined by the following equations [10].

$$M_o(t_o, t_f) = \int_{t_o}^{t_f} \hat{F}^T(t, t_o) \hat{C}^T(t) \hat{C}(t) \hat{F}(t, t_o) dt$$

$$M_c(t_o, t_f) = \int_{t_o}^{t_f} \hat{F}(t_f, t) \hat{B}(t) \hat{B}^T(t) \hat{F}^T(t_f, t) dt$$

Where \hat{F} is the system state transition matrix and \hat{B} and \hat{C} are time-invariant matrices defined earlier. A zero determinant is indicative of an unobservable or uncontrollable system.

Evaluation of the closed loop controller and observer eigenvalues is an alternative to the gramian matrix approach. The closed loop dynamics of each can be represented in state variable form as

$$\dot{\hat{x}} = [\hat{A} - K_2\hat{C}]\hat{x}$$

$$\dot{x} = [\hat{A} + BK_1]x$$

Maximizing the negative real parts of the eigenvalues is the configuration selection criteria which provides the most stable system possible. The eigenvalues are a direct indication of system controllability and observability. An eigenvalue with a zero or positive real part is indicative of an unstable system.

Results of the two methods correlate well which provides an easy and straight forward method for selection of actuator and sensor configurations. At this point in the design phase, the final configurations comprise the minimum amount of hardware for simplicity while assuring adequate system controllability and observability. Baseline actuator and sensor locations are shown in figure 1. The sensor and actuator complements that are used throughout the analysis portion of this study are listed in table 1.

LQG AND CLASSICAL CONTROL COMPARISON

The frequency and time responses from LQG and classical controllers will now be compared. The functional block diagram of the classical controller is shown in figure 2. This block diagram is in the form of a single input single output (SISO) system to control the center body rate and attitude. The open loop frequency responses of the classical controller are shown in figures 3 and 4. The gain plot in figure 3 clearly exhibits the low bandwidth in order avoid the first mode.

The multiple input multiple output (MIMO) frequency response of the rigid body rate and position states can be evaluated to provide a comparison of the capabilities of the two different controllers. The open and closed loop response of the LQG controller is shown in figures 5 and 6. The gain plot in figure 5 indicates a bandwidth which is almost an order of magnitude higher than that for a classical controller because of multiple leads near cross over. At structural frequencies, it is apparent that three modes are actively controlled and one mode, the second dominant mode, is notched from the controller due to that modes poor controllability and observability. One expects effects of this mode to be the most evident. Transient response, figures 7 and 8, of the center body and solar array angular position show that the LQG controller has a much faster response with a settling time less than 300 seconds while the classical controller requires more than 3000 seconds to settle. The extremely long settling time for the classical controller is indicative of it's inability to maintain precise attitude control when the spacecraft is influenced by outside disturbances such as payload or environmental torques. The quick transient response of the center body is performed at some expense of exciting the flexible modes while the classical controller accomplishes its objective since it does not excite any flexible modes. In fact, the difficult second dominant mode is the cause of the LQG controller oscillations beyond 200 seconds. Controllability and observability

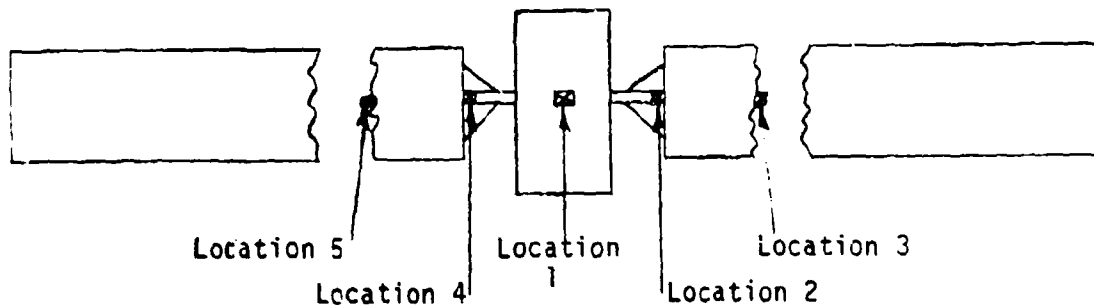


FIGURE 1. ACTUATOR AND SENSOR LOCATIONS

ELEMENT	LOCATION	TYPE
Actuator	1	Torque producing
Actuator	2	Torque producing
Actuator	4	Torque producing
Sensor	1	Angular rate
Sensor	1	Angular position
Sensor	2	Relative angular position (1)
Sensor	3	Relative angular position
Sensor	4	Relative angular position
Sensor	5	Relative angular position

Table 1. ACTUATOR AND SENSOR COMPLEMENT

Note 1. A relative position sensor measures local angular deflections relative to the center body.

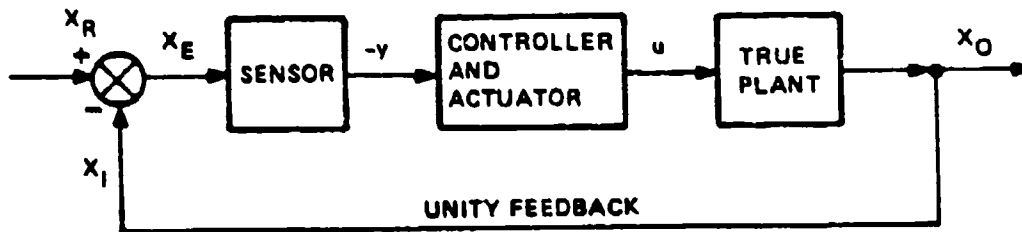


FIGURE 2. CLOSED LOOP SISO SYSTEM

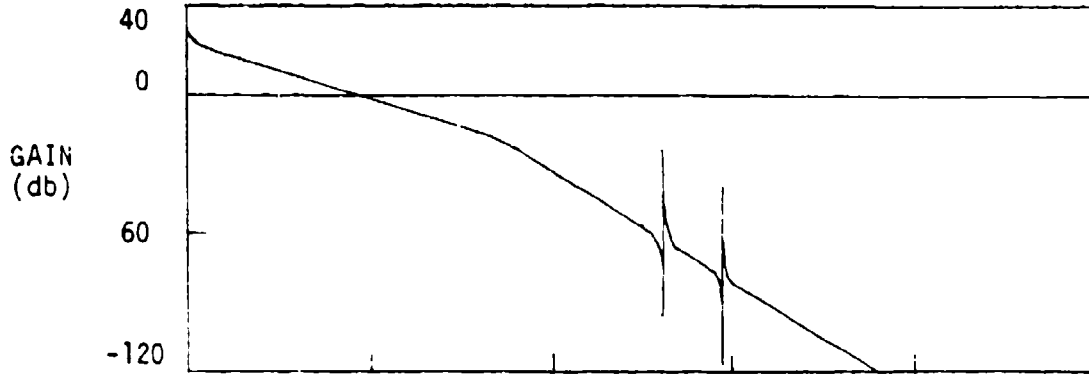


FIGURE 3. CLASSICAL CONTROLLER (OPEN LOOP GAIN)

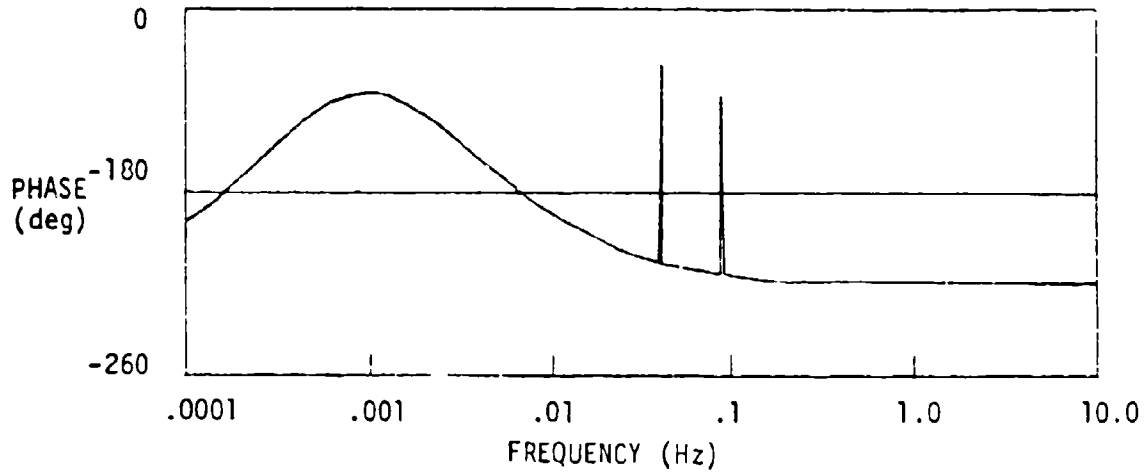


FIGURE 4. CLASSICAL CONTROLLER (OPEN LOOP PHASE)

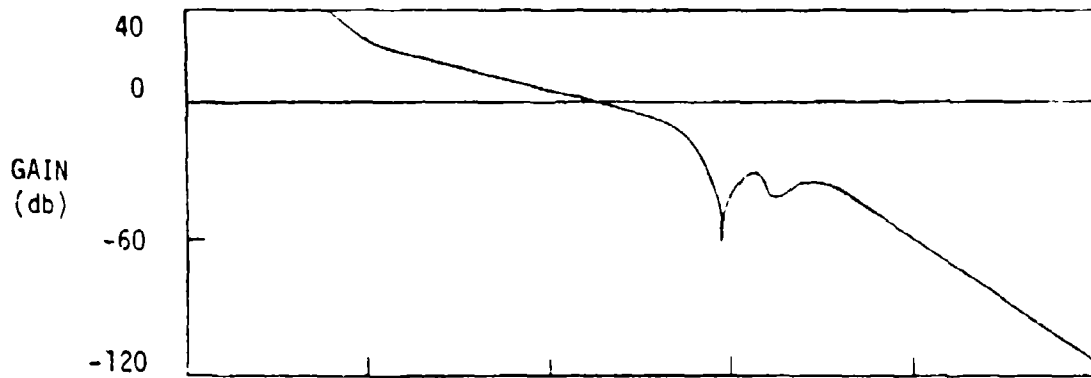


FIGURE 5. LQG CONTROLLER (OPEN LOOP GAIN)

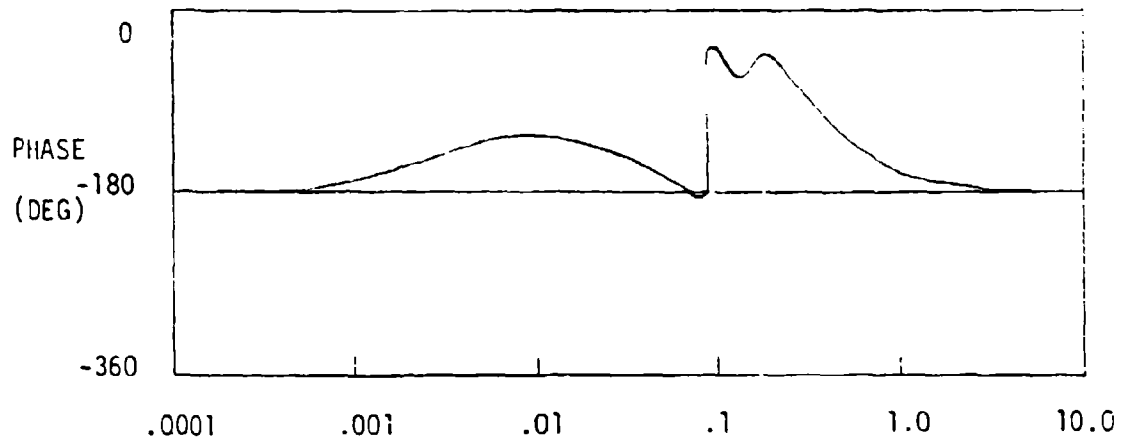


FIGURE 6. LQG CONTROLLER (OPEN LOOP PHASE)

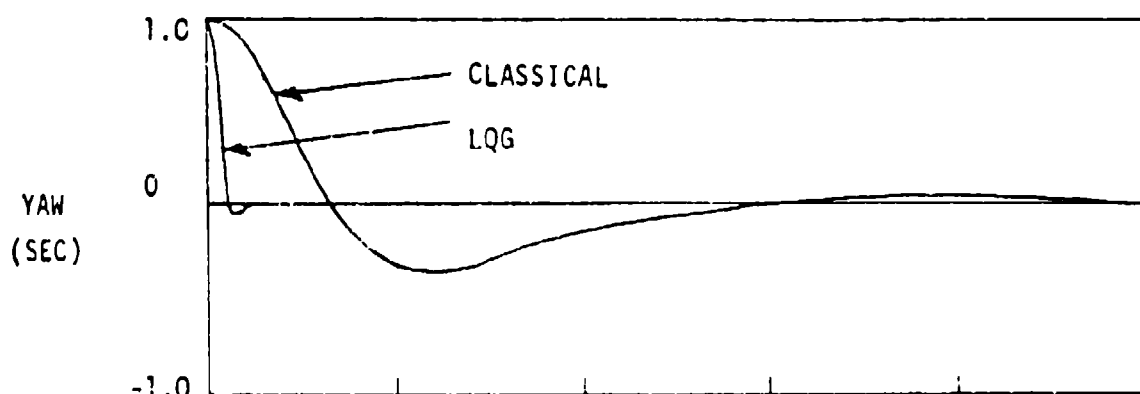


FIGURE 7. CENTER BODY TRANSIENT RESPONSE

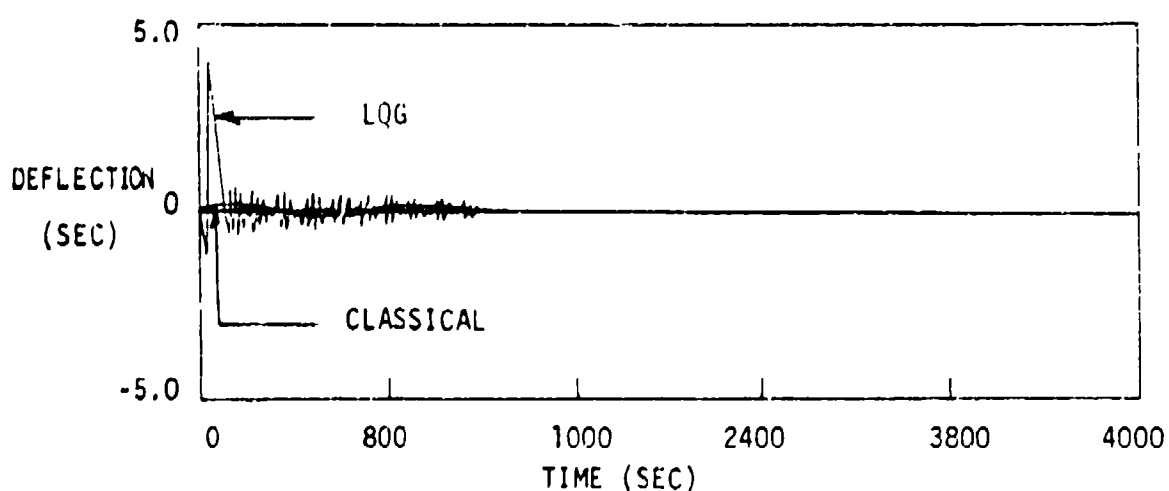


FIGURE 8. SOLAR ARRAY TRANSIENT RESPONSES

of this mode can be increased by adding, or to some degree relocating, sensors and actuators. Instead of increasing the complexity of the control system, we first investigate the advantages of adding passive damping in order to damp the second dominant mode.

EFFECTS OF PASSIVE DAMPING

The LQG controller gains are based on a very small damping ratio, 0.0005, for all flexible modes. This overly conservative and simplistic approach is taken to observe the capabilities of an LQG controller when, essentially, all damping had to be provided by the control system. Realistically, damping ratios will vary and are expected to be an order of magnitude greater which should make the controller design somewhat more stable than shown in these analyses. Indeed, this assertion is graphically depicted by figure 9. Stability of the controller increases with larger values for the damping ratio. The real part of the eigenvalue associated with the second dominant mode is a direct measure of stability and can be thought of as the effective system damping for that mode due to combined structure and controller damping. Transient response simulations, figure 10, also indicate a more stable system as the damping ratio is increased. However, increased damping reaches a point of diminishing return. Increased active modal control derived from damping ratios greater than .05 will require controller gain recalculation. So, it appears that active and passive damping trades can be made with performance and stability margins. This type of trade-off is certainly not new to system designers and it is encouraging to be able to quantify such trades in modern control theory applications.

FREQUENCY DOMAIN ANALYSES

Assuming the synthesis of an LQG controller leads to an acceptable system, a designer must then acquire control system margin and sensitivity information. Many studies during the last several years have shown that ROM controllers are sensitive to certain critical parameters [1]. Modelling errors of parameters such as damping ratios, modal natural frequencies, and modal admittances can invalidate whatever stability margins the designer thought existed in the approximated plant. Appropriate truncation of the distributed parameter system is also crucial to controller robustness for residual mode rejection. Further, inclusion of a particular mode in the ROM state space does not assure adequate modal control. Identifying problem modes early in the design phase is extremely useful for structure or passive damping design. All these concerns motivate development of analysis tools to show strengths and weakness of a control system design.

Most SISO controller designs rely heavily on frequency domain analysis (as well as frequency domain synthesis such as root locus [5]), but, these well known methods are currently in use only when system dynamics can be modelled in terms of scalar quantities and ordinary differential equations. A distributed parameter system with infinite modes is reduced (at some risk) to the major modes in order to simplify system dynamic models from partial to ordinary differential equations. This reduction allows the plant to be expressed as a finite MIMO system. Recent MIMO frequency response techniques draw parallels with SISO stability criteria in order to assure global stability over some

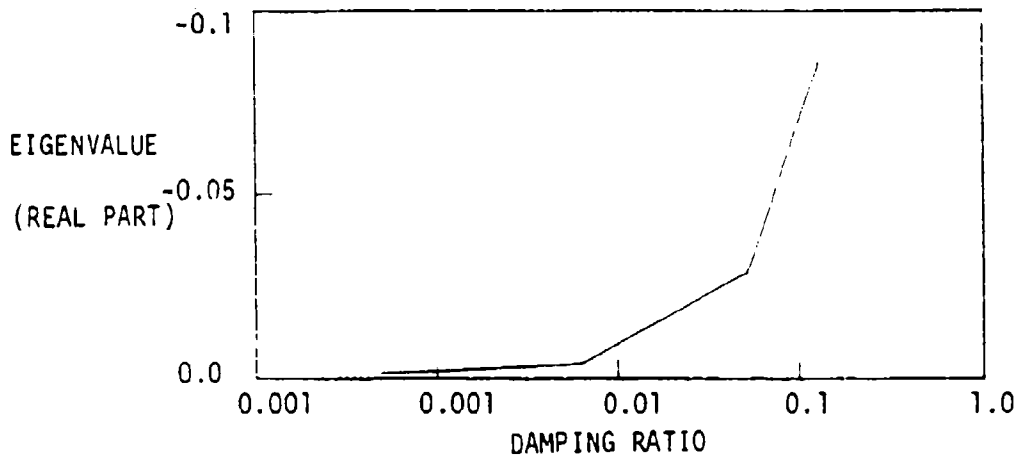


FIGURE 9. SECOND DOMINANT MODE STABILITY

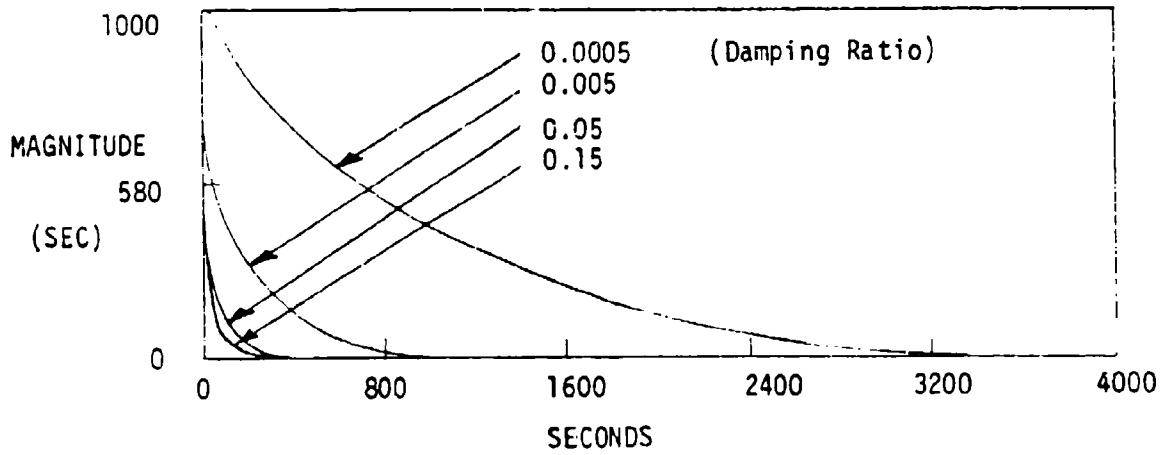


FIGURE 10. SECOND DOMINANT MODE TRANSIENT RESPONSE ENVELOPE

range of plant perturbations. Yet, these other MIMO techniques seem to give a stable/unstable indication at the system level with little insight into the stability or sensitivity of the state elements.

This paper presents results of frequency analysis methods that answer many of the stated concerns as well as provide insight into the state elements of a ROM controller. The examples highlight these capabilities and include simulation results to support frequency response predictions. One concludes that the frequency response analysis technique shown here is indeed useful and the wealth of information derived for SISO systems is applicable to MIMO systems as well.

FREQUENCY DOMAIN APPROACH

All frequency response analyses rely on development of the system transfer function. The concept of relating a systems output to the input, figure 11, is fundamental to system dynamics and feedback control. The MIMO open loop transfer function, G , is defined by

$$G = - (x_0/x_1)$$

where,

$$G = G(A, \hat{A}, B, \hat{B}, C, \hat{C}, K1, K2, j\omega)$$

Derivation of the system open loop transfer function is a straight forward time to frequency domain transformation with appropriate substitutions using equations (1) through (4). Open loop response requires loop closure of all states except the state of interest which results in a scalar transfer function. This transfer function is used to generate familiar Bode, Nyquist, and Nichols plots or other frequency domain type graphs which have been widely used for SISO analyses. Once the open loop response is obtained, the closed loop frequency response is easily calculated from the relation

$$g_{CL} = g_{OL} / (1 + g_{OL})$$

The following examples are intended to show the validity of this approach as well as some interesting applications.

EXAMPLE: NATURAL FREQUENCY ERROR TOLERANCE

LQG derived control and estimation gains are based on critical, a priori structure parameters such as modal natural frequencies. Errors in the assumed dynamics will result in non-optimal gain calculations such that system instability will eventually result as errors become too large. Tolerances to this type of error is essential because the true plant parameters are unknown to the control systems designer. Open loop gain and phase (Bode) plots for the second dominant mode are shown in figures 12 and 13. A characteristic 180 degree phase shift coincides with the peak in gain at the modal natural frequency. It is apparent from figure 13 that the phase margin of the system may be negative at .014 Hz (i.e. an 84% error). Therefore, one expects the system to be unstable if the natural frequency of this mode was overestimated

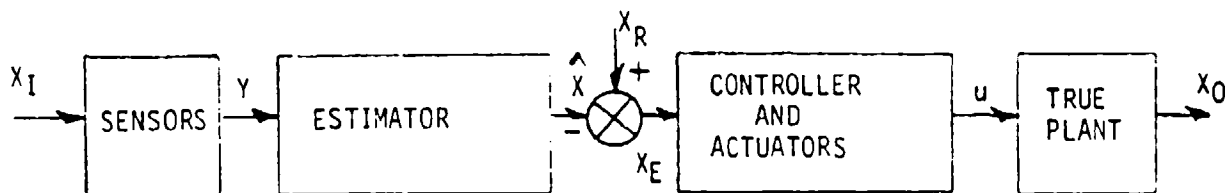


FIGURE 11. OPEN LOOP MIMO SYSTEM

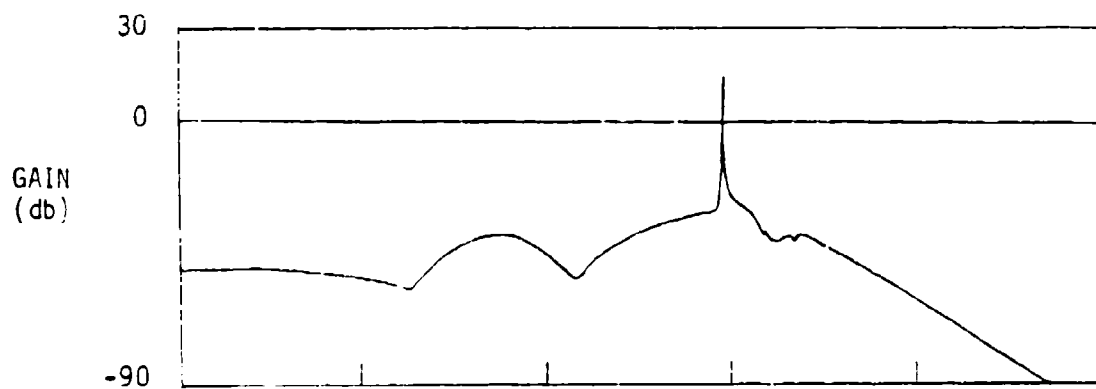


FIGURE 12. SECOND DOMINANT MODE OPEN LOOP GAIN

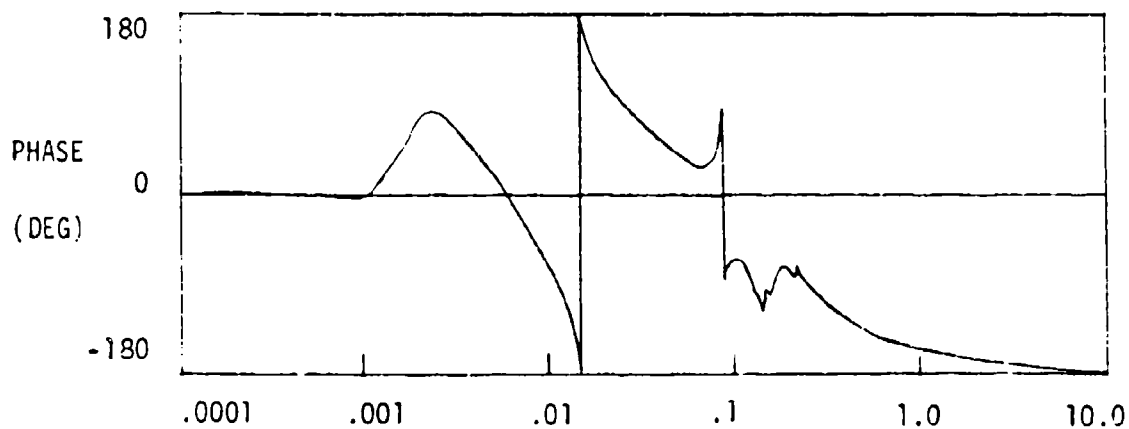


FIGURE 13. SECOND DOMINANT MODE OPEN LOOP PHASE

by some amount greater than 84%. Nyquist plots are very useful for modal analysis because of a modes characteristic circular contour when mapped onto the G plane. Nyquist stability criterion relates number of encirclements of the $-1 + j0$ point to system poles and zeroes in the right half plane. The Nyquist plot, figure 14 exhibits an encirclement of $-1 + j0$ with an 84% natural frequency error as expected from the Bode plots. Transient response simulations, figure 15, correlate very well with the Bode and Nyquist stability predictions that successful control is possible until the a priori second dominant modal frequency is overestimated approximately 84%. One should note from the Bode plots that underestimating this natural frequency will always result in a stable system due to some small amount of phase margin at higher frequencies.

EXAMPLE: MODAL ADMITTANCE ERROR TOLERANCE

Any ROM controller is susceptible to controller spillover. Two residual modes are included in the true plant for closer examination of this phenomenon. Figures 16 and 17 depict the Bode plots for the larger of these two residual modes. Closer inspection at the modal natural frequency shows a 27 DB of gain margin which at first glance appeared to be marginally stable. This is actually an indication of modal admittance error margin because the mode shape magnitude defines the height of this curve. In short,

$$\text{gain margin (DB)} = 20 \log(f(\phi^2))$$

where ϕ is the modal admittance. Working backward, one finds that 27 DB of gain margin equates to a factor of 4.73 error margin in the modal admittance values. Multiplying the admittances by 4.73 raises the gain curve so that the system is marginally stable due to zero gain and phase margins. Multiplying by a factor greater than 4.73 results in negative gain margin thus predicting system instability. Transient response simulations, figure 18, support the frequency response predictions.

CONCLUSIONS

The control synthesis and analysis techniques presented here will supplement other MIMO control system approaches to provide important capabilities for LSS control design. The performance advantages of LQG controllers for LSS are readily apparent. Precision pointing and quick transient response are very desirable attributes that an LQG controller can provide even with negligible structural damping.

However, to say the LQG controller can "do it all" oversimplifies the LQG controller synthesis problem. Constraints on number, location, and, accuracy of the actuators and sensors as well as onboard computational resource limitations will have to be considered early in the design. The designer may not have the desired flexibility in order to actively control all dominant modes. The inability to control the second dominant mode is a case in point. Simulations show that the center body can maintain precise pointing in spite of continued oscillation of the second dominant mode. This condition may be acceptable from a control system point of view, however, concerns with component or structure fatigue could render this design unacceptable thus

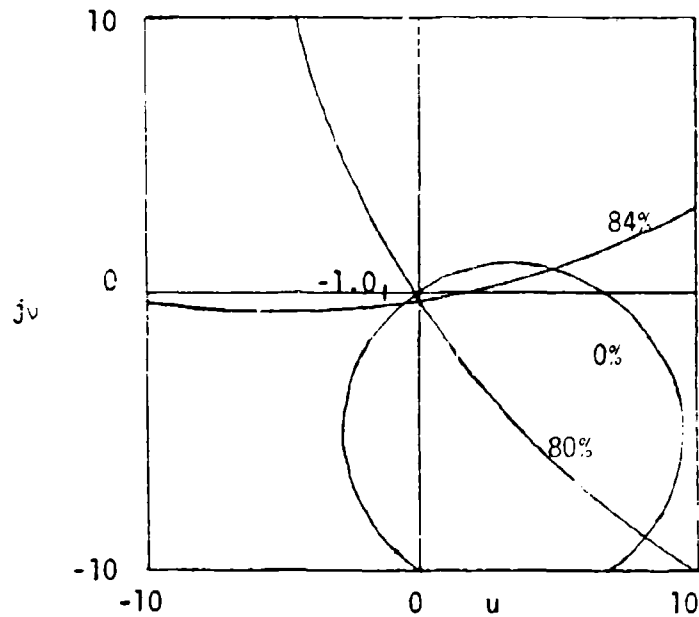


FIGURE 14. NYQUIST

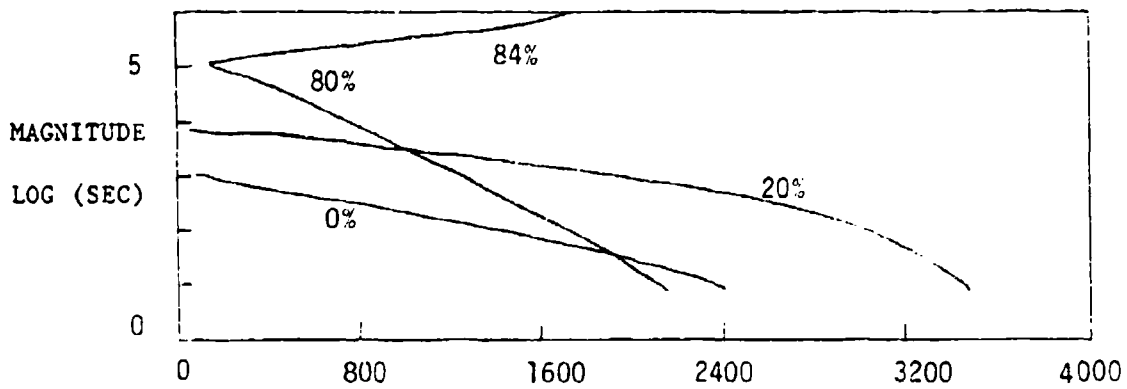


FIGURE 15. SECOND DOMINANT MODE TRANSIENT RESPONSE ENVELOPES

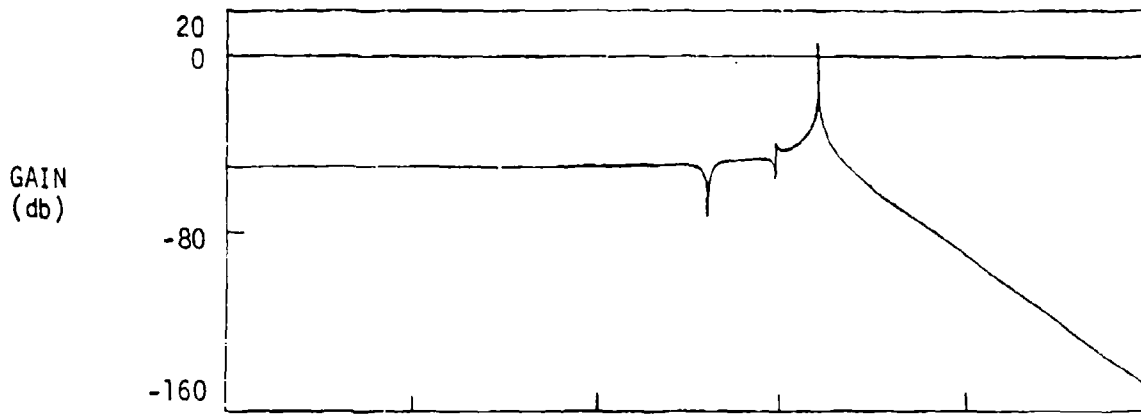


FIGURE 16. RESIDUAL MODE (OPEN LOOP GAIN)

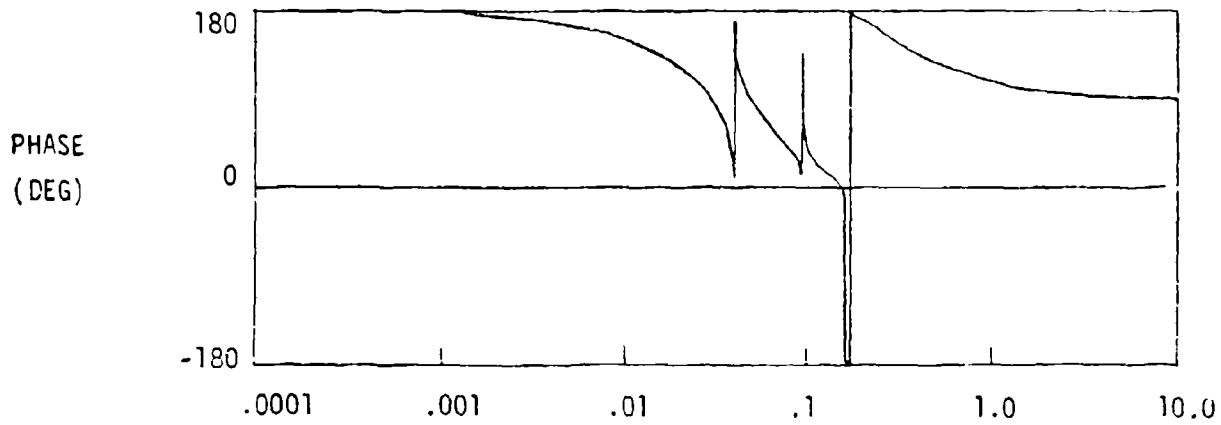


FIGURE 17. RESIDUAL MODE (OPEN LOOP PHASE)

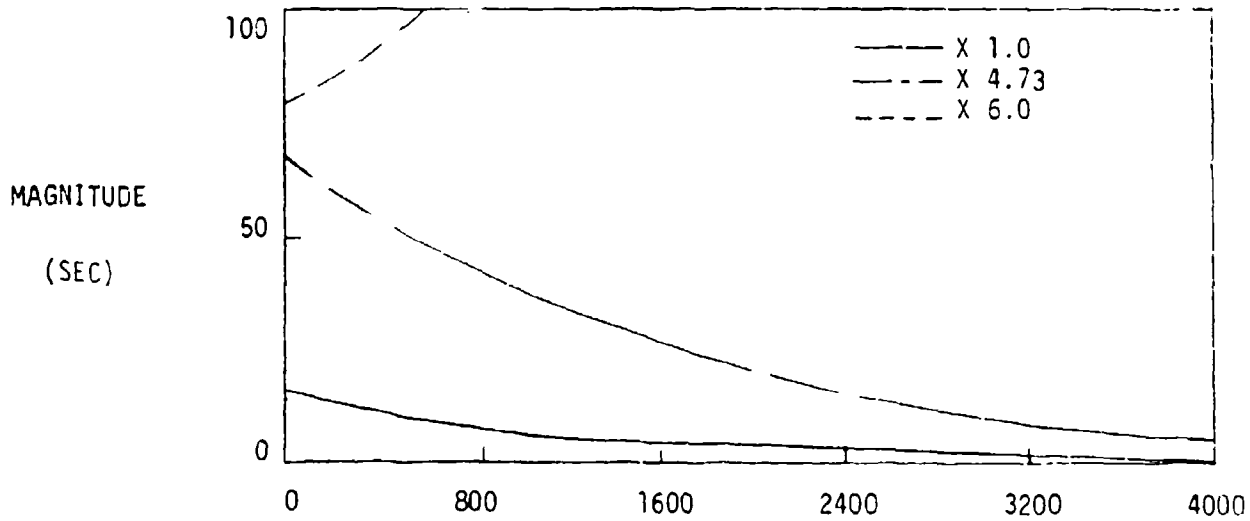


FIGURE 18. RESIDUAL MODE TRANSIENT RESPONSE ENVELOPE

establishing a requirement for passive damping in lieu of additional actuators and sensors for greater active control. Passive damping can also increase stability margins so that performance enhancements are possible.

System design trades to optimize cost, performance, and reliability as a combination of active and passive damping will require more detailed investigation as spacecraft requirements become identified. Development and further refinement of frequency response analyses such as the technique presented in this paper will become the tools to perform system trades necessary for successful LSS control system design.

References

1. Balas, M.J., "Trends in Large Space Structure Control Theory: Fondest Hopes, Wildest Dreams", IEEE Transactions on Automatic Control, Vol. AC-27, No. 3, June 1982.
2. Benhabib, R., et al, "Stability of Large Space Structure Control Systems Using Positivity Concepts", J. Guidance and Control, Vol. 4, No. 5, Sep.-Oct. 1981.
3. Bryson and Ho, "Applied Optimal Control", Blaisdell Publishing Co., 1969.
4. Chan, S. and Athans, M., "Applications of Robustness Theory to Power System Models", IEEE Transactions on Automatic Control, Vol. 29, No. 1, Jan. 1984.
5. Dazzo and Houpis, "Linear Control Systems Analysis and Design", McGraw Hill Inc., 1975.
6. DeCarlo, R., et al, "Multivariable Nyquist Theory", Int. Journal of Control, Vol. 25, No. 5, 1977.
7. Frame, J. and Garrett, S., "Robust Control: An Overview", IEEE Conference, CH1749-1/82.
8. Gelb, A. (Editor), "Applied Optimal Estimation", M.I.T. Press, 1974.
9. Postlewaite, I., et al, "Principal Gains and Principal Phases in the Analysis of Linear Multivariable Feedback Systems", IEEE Transactions Automatic Control, Vol. 26, No. 1, Feb. 1981.
10. Sage, A.P. and White, C.C., "Optimum Systems Control", 2nd Edition, Prentice-Hall Inc., 1977.